01 Jan 1965

Hot Isostatic Compaction of Graphite

Donald C. Carmichael

P. D. Ownby
Missouri University of Science and Technology, ownby@mst.edu

Edwin S. Hodge

P. D. Dunby

LEGAL NOTICE

Printed in USA. Price $1.00. Available from the Clearinghouse for Federal Scientific and Technical Information, National Bureau of Standards, U. S. Department of Commerce, Springfield, Virginia.

Report No. BMI-1746

UC-25 Metals, Ceramics, and Materials
(TID-4500, 45th Ed.)

AEC Contract W-7405-eng-92

HOT ISOSTATIC COMPACTION OF GRAPHITE

by

Donald C. Carmichael
P. Darrell Ownby
Edwin S. Hodge

October 5, 1965

BATTELLE MEMORIAL INSTITUTE
COLUMBUS LABORATORIES
505 King Avenue
Columbus, Ohio 43201

TABLE OF CONTENTS

HOT ISOSTATIC COMPACTION OF GRAPHITE

Donald C. Carmichael, P. Darrell Ownby, and Edwin S. Hodge

The effects of temperature, pressure, and graphite starting material on the density, isotropy, and strength of dense graphite material prepared by hot isostatic compaction of graphite powders were examined. Process equipment was developed to permit operation at temperatures up to 2700 C under a 1600-atom isostatic pressure of inert gas. The isotropy of graphite compacts was determined by neutron diffraction. Relatively isotropic, high-purity graphites were produced having modest isotropic tensile strength and extremely high density (up to 2.24 g per cm^3, or 99 per cent of theoretical).

INTRODUCTION

The properties of polycrystalline graphites depend strongly upon the method of manufacture. For most properties, such as conductivity, strength, and thermal expansion, this dependence results primarily from the extremely anisotropic properties of the constituent graphite crystallites. Theoretically, if the manufacturing process achieved crystallographically identical orientation of all crystallites, these polycrystalline properties would approximate those of the single crystal both in degree of anisotropy and magnitude of properties. At the other extreme, if all crystallites were randomly oriented during manufacture, these polycrystalline bulk properties would be isotropic and would be intermediate in magnitude between the directional extremes of the single crystal. These polycrystalline properties for actual products of manufacture have values between the orientation extremes. Properties such as bulk density, not related to the crystallite anisotropy, also depend strongly upon the manufacturing process.

Conventional, hot-working, and pyrolytic processes are used in the production of commercial polycrystalline graphites. While each of these processes may be varied to yield a range in product properties, each has limitations and yields a characteristic product. The conventional or traditional process by which most industrial graphite is manufactured consists basically of mixing carbon or graphite particles with a carbonaceous binder (such as pitch or resin), forming the mix to shape by extrusion or molding, baking to polymerize and carbonize the binder, and finally, graphitizing at high temperature (2500 to 3000 C). Because of the evolution of volatiles during baking, the conventional graphite inherently has high open porosity, relatively low density (<80 per cent of theoretical), and high permeability. Crystallite orientation ranges from slightly to moderately anisotropic. Hot working in its simplest form consists of uniaxially compressing a conventionally manufactured graphite at sufficiently high temperatures to plastically deform and densify it. The hot-worked product is highly anisotropic, dense (up to approximately 91 per cent of theoretical), and quite impermeable. Pyrolytic graphite is formed by the thermal decomposition of a carbonaceous gas on a heated substrate. In general, the product is characterized by extreme anisotropy, very low permeability, and high density.

Accumulating information on the effects of irradiation on polycrystalline graphites and the materials requirements of newer reactor concepts dictate graphite-property

combinations that are not satisfactorily attained by the present manufacturing processes.[1-3] Bulk dimensional stability of graphites under irradiation has been shown to be a strong function of the degree of anisotropy, and increasing evidence indicates that isotropic graphites exhibit maximum dimensional stability under neutron irradiation.[3] Graphite having very low permeability is of interest as a fuel matrix, cladding, or sleeve in order to control the escape of fission products in high-temperature gas-cooled reactors. There is, therefore, a need for graphite having the combination of minimum anisotropy and minimum permeability. None of the present manufacturing processes adequately achieves this property combination. Pyrolytic graphite is extremely impermeable but very anisotropic. Hot-worked graphite exhibits low permeability but is also anisotropic. Conventional graphite may be specially processed to approach isotropy and to achieve quite low permeability; however, this impermeability is associated with a "skin" region of maximum impermeability which is subject to damage, with an associated drastic increase in permeability.

The present program was undertaken to explore the applicability of the hot-isostatic-compaction technique developed at Battelle to the production of isotropic, high-density, impermeable graphite. This technique ideally provides many advantages for producing desirable property improvements:

(1) Extremely high densities are achieved by the simultaneous application of high pressures and high temperatures.

(2) The isostatic application of pressure virtually eliminates a major characteristic of conventional forming processes, the particle orientation caused by the forming process itself.

(3) The process can be used to produce a final product in one forming step without requiring subsequent graphitization at higher temperatures.

(4) Specimens of complex geometry can be directly formed.

MATERIALS

Graphite Powders

In order that the properties of a wide assortment of graphite powders and their response to this unique densification process might be investigated, materials ranging from relatively low-purity, naturally occurring graphites, to high-purity, highly refined, spectrographic-grade graphites were selected.

Natural Graphites

The natural graphites were obtained in powder form from The Asbury Graphite Mills, Inc. The analysis, as obtained from Asbury, is given on the next page for each type of natural graphite.

(1) References at end.

	Vendor's Analysis, w/o				
	Mexican	Norwegian	Ceylonese	Madagascan	German
Carbon	85.16	90.00	98.50	99.9	~90
Moisture	None	0.14	0.05	--	--
Volatiles	1.50	1.23	0.75	--	--
Ash	13.34	8.63	0.80	--	--

The ash is composed of approximately 50 w/o SiO_2, 25 w/o Al_2O_3, 10 w/o iron oxide, and 15 w/o sulfur and oxides of magnesium, calcium, sulfur, potassium, and sodium. Although the German grade was supposedly over 99.90 w/o carbon, approximate analysis indicated significant amounts of impurities.

Artificial Graphite

A 99.9 w/o carbon, artificially graphitized powder, with a 0.1 w/o ash mainly composed of CaO and TiO_2 (approximately 0.03 w/o each) was obtained from the Asbury Mills. This material was analyzed by X-ray diffraction at Battelle and found to have a graphitic structure.

Spectrographic Graphite

Very-high-purity, spectrographic-grade graphite of 99.99 w/o carbon was obtained from Ultra Carbon Corporation. This material had been purified by the Ultra "F" process and was spectrographically analyzed with good sensitivity by Ultra as follows:

	Results of Vendor's Successive Spectrographic Analyses[a]		
	A	B	C
Aluminum	0	0	0
Boron	X	X	X
Calcium	X	X	X
Copper	X	X	X
Iron	X	X	0
Magnesium	1	1	2
Manganese	X	X	X
Silicon	1	0	0
Sodium	X	X	X
Potassium	X	X	X
Tin	X	X	X
Titanium	X	X	X
Vanadium	X	X	X
Lead	X	X	X
Zinc	X	X	X

(a) Code used:
X = absent
0 = barely visible
Numbers indicate relative intensity.

X-ray diffraction analysis of this material indicated a graphite structure

Moldable Powders

Basic Carbon Corporation's Moldable Graphite MG-2 and Moldable Carbon MC-2 were used to compare the properties achieved from commercial molding mixtures with those prepared from the "raw" powders. The supplier's typical analyses follow:

	Vendor's Analysis, w/o	
	MG-2 (Graphite Powder + 20 w/o Organic Binder)	MC-2 (Carbon Powder + 18 w/o Organic Binder)
Carbon	95	95
Hydrogen and oxygen	4	4
Ash	0.5	0.5

Spherical and Irregularly Shaped Pyrolytic Particles

In order to investigate the effect of spherical particles on the isotropy of the final product, 400-μ pyrolytic-carbon spheres were produced by deposition of carbon on 100-μ coke particles by a fluidized-bed technique. As a second pyrolytic-powder material, pyrolytic-graphite machining fines were obtained from Super-Temp Corporation

Container Materials

Compaction containers were fabricated entirely from seamless tantalum tubing The majority of the containers were fabricated from 0.625-in -OD, 0 020-in. -wall tubing cut into lengths ranging from 1.00 to 2 75 in The ends of the containers were cut from rod into approximately 0 125-in. -thick plugs and electron-beam welded to the tubing. Tantalum was chosen as the container material because of its ability to form gastight, reliable welds, its good deformation characteristics over a wide temperature range, and its having the highest metal-carbon eutectic temperature (2800 C) of the available container materials.

HOT-ISOSTATIC-COMPACTION PROCESS

The hot isostatic compaction of powders first involves the vacuum sealing of the powders to be densified into pressuretight metal envelopes. The envelopes are of the general geometry of the desired hot-pressed specimen The envelope containing the powder is placed in a furnace that is inside a high-pressure autoclave. The furnace is then heated to an elevated temperature while the autoclave is being pressurized to a high pressure with an inert gas. The gas pressure is uniformly transmitted through the walls of the metal container (which have become soft at the elevated temperature) to isostatically hot press or compact the powder. This process, originally developed for the cladding of fuel elements has been applied to the consolidation of a variety of powder materials.[4, 5] Further description of the equipment is also available in the literature.[6]

High-Pressure Autoclave

The autoclave unit used for these studies was designed for an internal pressure of 3,400 atm (50,000 psi). This vessel, as shown in Figure 1, has a 9-in. ID by 60-in. inner length. and was machined from a modified 4340 steel forging. While the unit is in operation, coolant oil is pumped at approximately 12 gal per min through a coolant jacket with spiral baffles which covers the entire length of the vessel. Separate coolant is also pumped through the upper head and through the upper and lower electrode assemblies.

Furnace

A helical graphite resistance element was designed for the autoclave unit for operation to 2800 C. The element was machined from a graphite tube 3 in. in ID, 4 in. in OD, and 56 in. long. The graphite heater unit was installed into the autoclave, as illustrated in Figure 2. Concentric tubes of graphite and carbon with layers of carbon cloth between serve as insulation for the vessel wall. Because of the high thermal conductivity of the helium gas and the porosity of these materials, the thermal-insulation value is poor. Helium gas, in spite of its higher thermal conductivity, proved to be preferable to argon, which caused overheating of the upper portion of the vessel. This overheating of the upper cover area when using argon gas occurs because the high density of the gas causes a greater thermal convection, which offsets the advantage of having the lower thermal conductivity. The gap between the graphite heater tube and the graphite insulation tube is closed with a fused quartz plate. This plate opening must be precision machined to prevent hot gas from flowing between the two tubes, and yet allow for the differences in thermal expansion. The flow of hot gas up the center of the heater tube is inhibited by the use of disks of graphite, carbon, and carbon-felt materials and a steel plug. Perforated disks of graphite and carbon reduce radiant heat losses through the bottom of the heater tube.

Four sheathed Chromel-Alumel thermocouples are located at various critical points within the top of the vessel to determine possible overheating. The cycle is aborted if there is any indication of overheating in these areas.

An external gas bypass is necessary in order to maintain a balance of pressure within the heater and the top cavity just below the upper covers. This pressure differential is most significant during the first few minutes of heatup.

The current circuit proceeds from the insulated top electrode assembly, through the graphite heater tube that heats the grooved portion, then through the bottom electrode assembly to complete the circuit.

The power is supplied to the graphite heater from a 240-v, single-phase, 75-kva line through a saturable-core reactor to an impedance-matching 4-to-1 isolation transformer. In the present study, the limit of those present power capabilities has been reached utilizing the full 75 kva to achieve the extreme conditions required. To carry this high current, four Size 0000 flexible motion-picture cables are used for each electrode. Figure 3 shows the location of these electrodes and cables on the top cover of the autoclave. Low-voltage transmission losses have been minimized by setting the isolation transformer close to the autoclave.

23159

FIGURE 1. VIEW OF THE 9-IN.-ID AUTOCLAVE WITH A 60-IN. INNER LENGTH DESIGNED FOR OPERATION AT 3400 ATM (50,000 PSI)

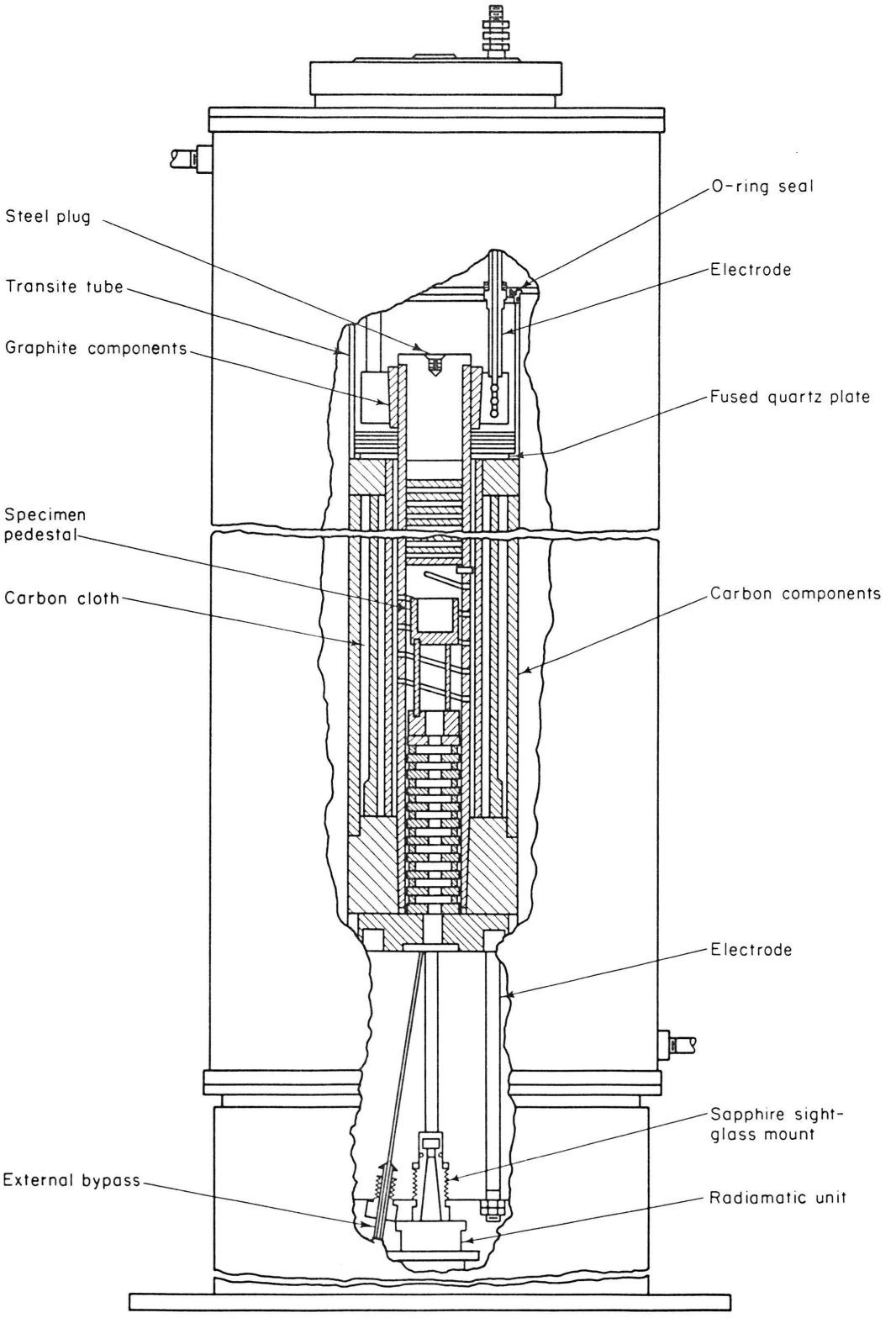

FIGURE 2. HIGH-PRESSURE AUTOCLAVE WITH GRAPHITE HEATER

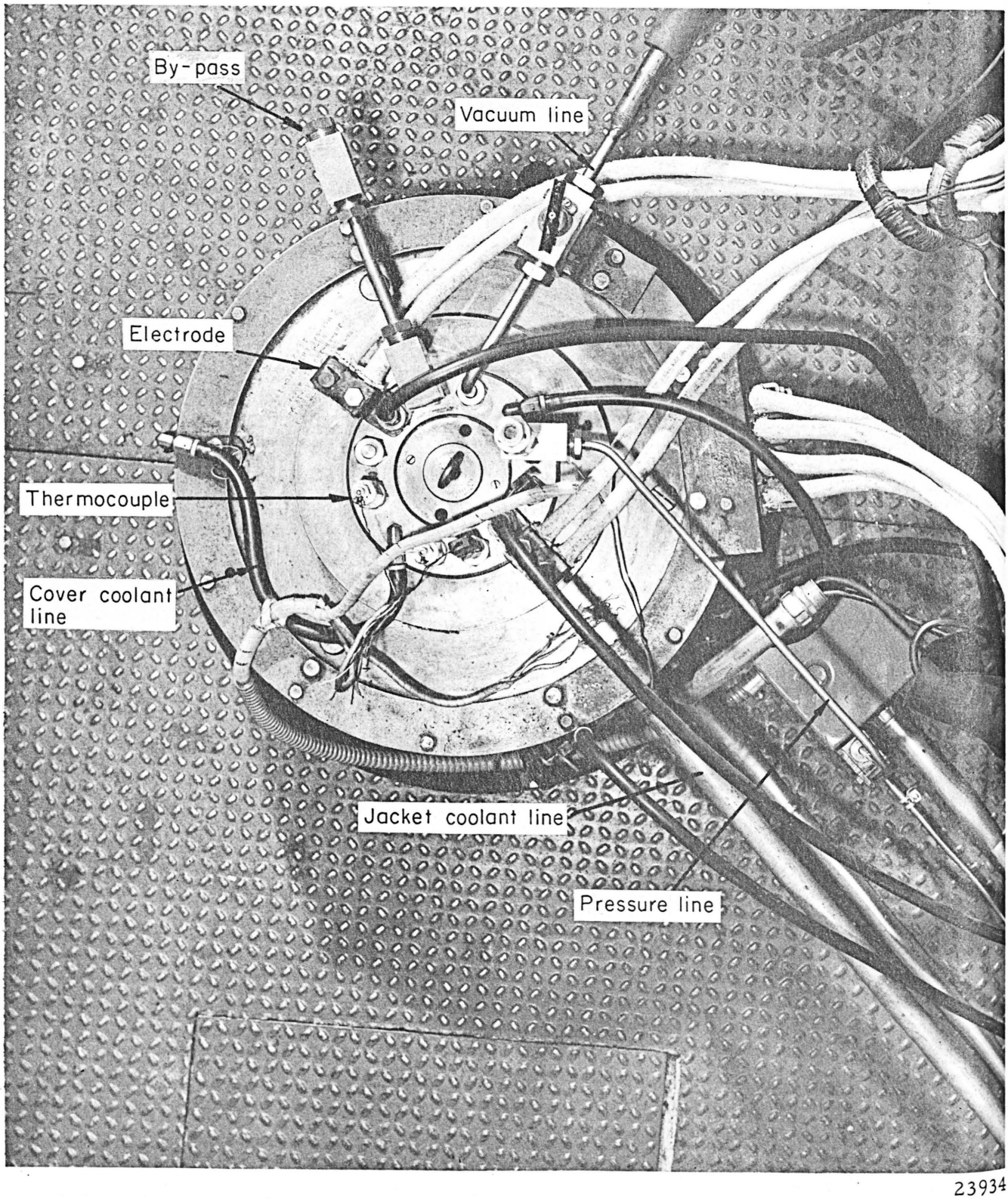

FIGURE 3. TOP VIEW OF THE HIGH-PRESSURE AUTOCLAVE UNIT

Compressor

The pressure for the autoclave unit is supplied by a 1020-atm (15,000-psi) multistage piston compressor and a 2450-atm (36,000-psi) booster compressor with a capacity of 950 standard ft^3 per hr. To minimize the gas movement within the autoclave, thus providing more stable operation, the vessel is pressurized before heating.

Specimen Location and Temperature Measurement

The specimens to be compacted are placed into a graphite crucible mounted on a pedestal made of graphite rods, as illustrated in Figure 2. Temperature measurements are made on the bottom of this crucible through a sapphire sight glass with a Brown Radiamatic unit, as shown in Figure 4. The Radiamatic unit converts the radiant energy to a voltage which is read out on a Honeywell Universal Recorder-Controller which allows both manual and automatic control of the heater. The unit is attached to the vessel by a precision-hinged mount so that it can be moved to one side for visual observations into the heater. This is accomplished by the use of a chain of front-surface mirrors forming an open periscope.

Investigations in the operation of the autoclave unit are being continued to improve temperature measurements, minimize heat losses in order to extend cycle time, and extend the uniform hot zone.

PROCEDURES AND PROCESS DEVELOPMENT

Powder Preparation

Sizing and Mixing

The various powders, with the exception of the pyrolytic and moldable powders, were screened into the following Tyler series mesh-size fractions: minus 100 plus 200, minus 200 plus 325, minus 325, and <1 μ. Wider particle-size distributions were obtained by mixing these narrower fractions. The mixtures were made on the basis of McGeary's studies of mixtures of various monosized spheres.[7] In order that some reasonably good size distributions could be obtained for the production of high-density material, McGeary's ideal systems were used as a basis for the relative amounts of the size fractions mixed, although the graphite powders deviated greatly from the ideal. Quaternary, ternary, and binary mixtures of particle-size ranges as well as single-size-range specimens were made.

Mixing was accomplished by a rolling-mill technique. It was found necessary to add 1 to 8 w/o paraffin as binder to the artificial graphite in order for it to hold together after cold hydrostatic pressing. The pyrolytic-carbon spheres and moldable powders were used as received. Paraffin binder was added to the pyrolytic-graphite machining fines.

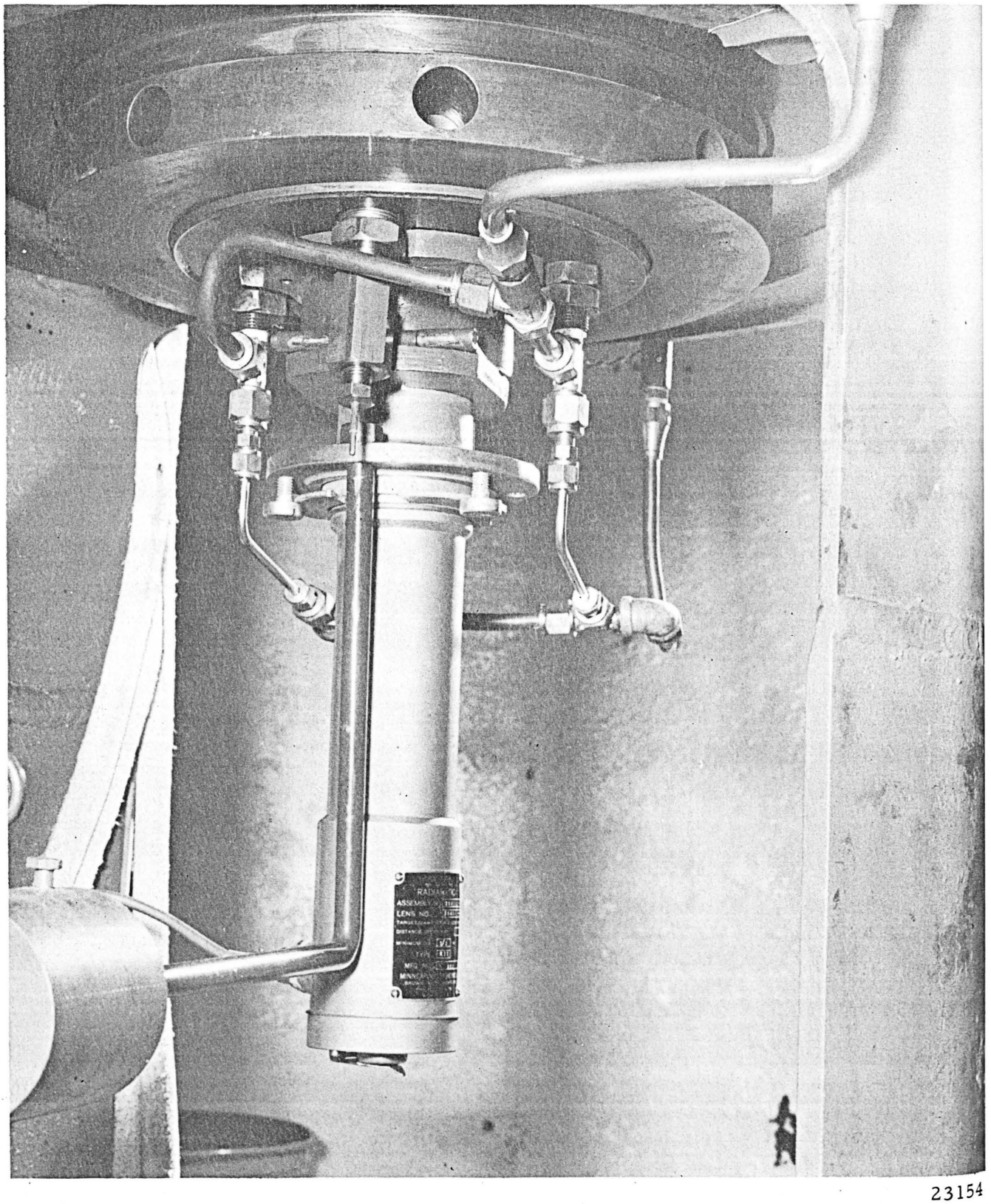

23154

FIGURE 4. BROWN RADIAMATIC UNIT USED TO MEASURE THE TEMPERATURE IN THE HIGH-PRESSURE AUTOCLAVE WITH THE GRAPHITE HEATER

Cold Hydrostatic Pressing

The powders were tamp-packed into rubber bags which were externally supported by metal tubing. The rubber bags were then evacuated and sealed and cold hydrostatically pressed at 100,000 psi. This procedure worked well on all but the pyrolytic-graphite powders which would not hold together after cold pressing. After the first structural orientation tests were made, it was found that the basal (002) planes of the spectrographic grade of graphite powders were oriented perpendicular to the direction of tamping during the loading of the rubber bags, so all subsequent loadings on these powders were carried out without tamping, and the isotropy of the final specimens was significantly improved.

Specimen Preparation

The cold-pressed specimens were removed from the rubber bags and shaved down to closely fit the tantalum containers. The pyrolytic-graphite powders could not be cold pressed and were simply poured into the tantalum cans, as were the spherical carbon particles. Also, for density comparisons with hydrostatic pressing, some powders were tamp-packed into containers directly. The graphites were all outgassed at conditions ranging from 200 C for 4 hr in air to 850 C in vacuum for 1/2 hr. The higher outgassing temperatures were used for the artificial graphite to burn out all the paraffin binder.

Furnace Calibration and Loading Geometry

At high temperatures (>2500 C) the pressure in the autoclave had a significant effect on the temperature indicated by the Brown Radiamatic pyrometer. Apparently the higher gas density at higher pressures (>1000 atm) causes the Radiamatic unit to read low at very high temperatures, thus causing melting of specimens and containers. In addition to the error due to the dense gas through which the Radiamatic unit must sight, sighting is focused on the bottom of the graphite plate which supports the specimens (see Figure 2). The temperature gradient in the specimen hot zone from top to bottom was also of interest since only the bottom temperature is seen by the Radiamatic. The Radiamatic readings were therefore calibrated with the eutectic melting points of three refractory metal-carbon systems: molybdenum (~2200 C), tungsten (~2710 C), and tantalum (~2800 C).

The approximate calibration was accomplished by placing pieces of foil of each of the three refractory metals on each of three graphite disks. The foil pieces were separated and were each in contact with the graphite-disk holders which supported them at different levels. After a calibration run, the temperatures achieved could be approximated by observing which metals appeared to be melted at the various levels along the hot zone, knowing the metal-carbon eutectic temperatures, and neglecting the relatively small pressure effects.

The calibration experiments indicated that reasonably constant temperatures existed in a hot zone 2-1/4 in. in diameter by 2 in. in length between 2200 and 2800 C in the 680 to 1360-atm range. In addition, there was evidence that at pressures as high as 1360 atm the Radiamatic unit reading 2200 C reads ~500 C low, whereas at pressures

up to 680 atm its reading is reasonably accurate. Subsequent experimental runs indicated that at 850 atm (12,500 psi) the Radiamatic unit could read 2650 C (150 C below the tantalum-carbon eutectic at 2800 C) for 1-hr soak without melting the tantalum containers. Therefore, the error due to higher pressures seems to be relatively small up to 850 atm.

The hot zone in the graphite heater used for this program was limited to a length of ~2 in. at high temperatures and pressures. The furnace inside diameter is approximately 2.5 in. Experimental specimens were therefore usually limited to 1 in. in length and placed on a pedestal of such a length as to be in the center of the zone. Specimens were wrapped in 0.005-in. tantalum foil as protection against oxidation because of impurities in the autoclave gas.

Container Removal

After hot isostatic compaction the tantalum-canned specimens deformed typically, as shown in Figure 5.

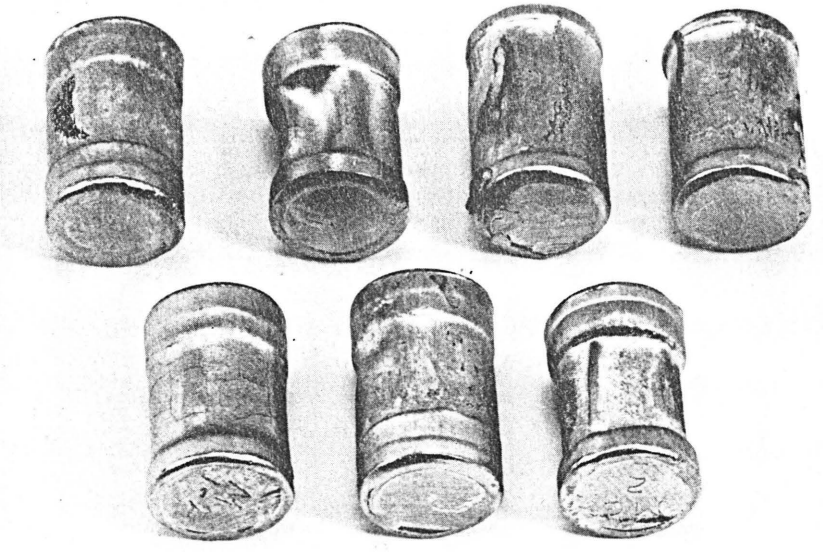

1X 20350

FIGURE 5. TYPICAL APPEARANCE OF TANTALUM-CANNED GRAPHITE SPECIMENS AFTER HOT ISOSTATIC COMPACTION

The containers were removed from the specimens by either cutting them with an abrasive wheel or pickling in HF. The HF treatment had no apparent deleterious effect on the specimens.

SPECIMEN-EVALUATION METHODS AND RESULTS

In order to obtain strength measurements on these small experimental specimens, the diametral loading technique, described later in this section, was used. Since this technique requires specimens of short, right cylindrical geometry, the compacted specimens were machined to a diameter of 0.35 in. and a length of 0.35 in. These uniform specimens were then used to carry out the various property measurements.

Density Measurements

Standard density-measurement techniques, including mercury- and water-displacement pycnometry, were used to evaluate the density of the specimens. The density measurements before hot isostatic compaction consisted of simple measurements of the weight of the specimen and the volume of the container. This technique was also used on the hot-isostatically-compacted specimens after they were machined to uniform size. Precise dimensional and weight measurements could then be made on each specimen. These measurements yielded densities which correlated well with the best values from the other techniques.

The densities and particle-size distributions of the cold-hydrostatically-pressed specimens of the various graphites are tabulated in Table 1. In general, very high densities were achieved by cold hydrostatic pressing. The hot-isostatically-compacted densities are given in Table 2 which shows the effects of hot pressing on the various types of graphites, and the temperatures and pressures of compaction. The densities of commercial graphites obtained for comparison range typically from about 70 to 90 per cent of theoretical density.

Metallographic Examinations

Metallographic examinations of the specimens were performed (1) to give an approximate check on the measured density value, (2) to characterize the structure by observing the size and shape of the grains, and the presence and distribution of other phases, if any, and (3) to detect obvious orientation effects.

Electrolytic etching techniques described by Tarpinian[8, 9] have proven to be of great value in elucidating the graphite structure. The etchant, composed of 80 ml of H_3PO_4, 60 ml of H_2O, 16 g of $K_2Cr_2O_7$, and 1 g of $FeCl_3$, was used with a direct current at 6 v. Fine, detailed structures are revealed by this technique.

A representative microstructure of a conventionally fabricated reactor-grade graphite is presented in Figure 6 for comparison with Battelle-fabricated graphites. Hot-isostatically-compacted specimens of three natural-graphite powder materials are represented in Figures 7 through 9. A series of the compacted specimens of the very pure spectrographic-grade graphite is presented in Figures 10 through 13, showing the effects of the compaction conditions and the very-high-density material obtained at all except the lowest compaction conditions used. The generally high densities achieved and the structures of the compacted artificial-graphite material of high purity are illustrated in Figures 14 and 15.

TABLE 1. EFFECT OF TYPE OF MATERIAL AND PARTICLE SIZE ON DENSITIES OF COLD-COMPACTED GRAPHITES[a]

Specimen	Mesh-Size Range (Tyler Series), w/o: Minus 100 Plus 200	Minus 200 Plus 325	Minus 325	<1μ	Density Before Hot Isostatic Compaction: G per Cm^3	Per Cent of Theoretical[b]
Spectrographic-Grade Graphite (99.99 w/o Carbon)						
100	100	--	--	--	1.32	58
200	--	100	--	--	1.21	53
325	--	--	100	--	1.01	45
U-1	100	--	--	--	2.11	93
U-2	--	100	--	--	2.02	89
U-3	--	--	100	--	2.04	90
U-4	--	--	--	100	1.90	84
U-5	62.5	37.5	--	--	2.09	92
U-6	62.5	--	37.5	--	2.03	90
U-7	62.5	--	--	37.5	1.96	86
U-8	--	62.5	37.5	--	1.74	77
U-9	--	62.5	--	37.5	1.96	87
U-10	--	--	62.5	37.5	1.77	78
U-11	62.5	23.1	14.4	--	2.01	89
U-13	--	62.5	23.1	14.4	2.07	91
U-Q	62.5	18.6	11.6	7.3	2.05	91
U-13L	--	43.0	47.0	10.0	1.83	81
Artificial Graphite[c] (99.9 w/o Carbon)						
A-1	100	--	--	--	1.34	59
A-3	--	--	100	--	1.48	65
A-4	62.5	37.5	--	--	1.40	62
A-5	--	62.5	37.5	--	1.40	62
A-6	62.5	--	37.5	--	1.46	64
AGL	62.5	--	37.5	--	1.46	64
A-7	62.5	23.1	14.4	--	1.51	67
Pyrolytic Graphite[c,d]						
PY-5	--	--	--	--	0.96	42
PY-6	--	--	--	--	1.30	57
PY-7[e]	--	--	--	--	1.20	53
Madagascan Natural Graphite (99.90 w/o Carbon)						
Ma-1	62.5	18.6	11.6	7.3	2.12	94
Ma-2	62.5	23.1	14.4	--	2.25	99
Ma-3	--	62.5	23.1	14.4	2.14	94
Ma-4	--	62.5	37.5	--	2.10	93
Ma-5	--	--	62.5	37.5	2.09	92
Ma-6	--	100	--	--	2.12	94
Ma-7	--	--	100	--	2.14	95
Ma-8	100	--	--	--	2.14	95
German Natural Graphite (~90 w/o Carbon)						
G-1	100	--	--	--	2.21	98
G-2	--	100	--	--	2.24	99
G-3	--	--	100	--	2.26	100
G-4	62.5	37.5	--	--	2.26	100
G-5	--	62.5	37.5	--	2.27	100
G-6	62.5	--	37.5	--	2.23	98
G-7	62.5	23.1	14.4	--	2.23	98

TABLE 1. (Continued)

Specimen	Mesh-Size Range (Tyler Series), w/o: Minus 100 Plus 200	Minus 200 Plus 325	Minus 325	<1 μ	Density Before Hot Isostatic Compaction: G per Cm³	Per Cent of Theoretical[b]
Ceylonese Natural Graphite (98.50 w/o Carbon)						
C-1	62.5	18.6	11.6	7.3	2.07	91
C-2	62.5	23.1	14.4	--	2.12	94
C-3	--	62.5	23.1	14.4	2.09	92
C-4	--	62.5	37.5	--	2.02	89
C-5	--	--	62.5	37.5	1.97	87
C-6	--	100	--	--	2.15	95
C-7	--	--	100	--	2.11	93
Norwegian Natural Graphite (90.00 w/o Carbon)						
N-1	100	--	--	--	2.25	99
N-2	--	100	--	--	2.10	93
N-3	--	--	100	--	2.10	93
N-4	62.5	37.5	--	--	2.24	99
N-5	--	62.5	37.5	--	2.17	96
N-6	62.5	--	37.5	--	2.19	97
N-7	62.5	23.1	14.4	--	2.15	95
Mexican Natural Graphite (85.16 w/o Carbon)						
M-1	62.5	18.6	11.6	7.3	1.63	72
M-2	62.5	23.1	14.4	--	1.64	73
M-3	--	62.5	23.1	14.4	1.72	76
M-4	--	62.5	37.5	--	1.77	78
M-5	--	--	62.5	37.5	1.70	75
M-6	--	100	--	--	1.63	72
M-7	--	--	100	--	1.48	65
M1-2	62.5	18.6	11.6	7.3	1.59	70
M2-2	62.5	23.1	14.4	--	1.61	71
M3-2	--	62.5	23.1	14.4	1.71	76
M4-2	--	62.5	37.5	--	1.72	76
Moldable Carbon and Moldable Graphite Powders (95 w/o Carbon)						
MC-2	Particle-size analysis unknown				1.42	63
MG-2	Particle-size analysis unknown				1.65	73
Pyrolytic Carbon Spheres (400 μ)						
					1.13	50

(a) Except for Specimens 100, 200, 325, and the pyrolytic specimens, all specimens were compacted by hydrostatic pressing at 100,000 psi. The exceptions were tamp packed.

(b) Calculated assuming 100 per cent graphite, using 2.265 g per cm^3 as theoretical density.

(c) The lower densities of the pyrolytic and artificial graphites are partly due to the 1 to 8 w/o paraffin added as a cold-compaction aid.

(d) Estimated size range was minus 60 plus 325 mesh.

(e) Pyrolytic artificial graphite powder mixture.

TABLE 2. DENSITIES OF COLD-PRESSED GRAPHITES THAT WERE HOT ISOSTATICALLY COMPACTED

Specimen[a]	Density After Cold Hydrostatic Pressing		Density After Hot Isostatic Compaction	
	G per Cm^3	Per Cent of Theoretical	G per Cm^3	Per Cent of Theoretical
Isostatically Hot Pressed at 1650 C and 680 Atm for 2 Hr				
M-4	1.77	78	1.84	81
M-6	1.63	72	1.91	84
U-3	2.04	90	2.08	92
Isostatically Hot Pressed at 1750 C and 1090 Atm for 2 Hr				
M-3	1.72	76	1.95	86
N-2	2.10	93	2.18	96
Ma-4	2.10	93	2.14	94
Isostatically Hot Pressed at 1950 C and 2040 Atm for 2 Hr				
U-2	2.02	89	2.18	96
M-1	1.63	72	2.03	90
M-2	1.64	73	2.12	93
N-7	2.15	95	2.24	99
C-7	2.11	93	2.15	95
Isostatically Hot Pressed at 2500 C and 440 Atm for 2 Hr				
U-7	1.96	86	2.19	97
MC-2	1.42	63	1.82	80
MG-2	1.65	73	1.87	82
A-3	1.48	65	1.95	86
M-7	1.48	65	1.67	74
Ma-6	2.12	94	2.19	97
Isostatically Hot Pressed at 2700 C and 820 Atm for 1 Hr				
C-5	1.97	87	2.09	92
U-6	2.03	90	2.15	95
A-6	1.46	64	2.10	93
MG-2	1.65	73	1.91	84
U-13LA[b]	1.83	81	2.15	95
U-13LB[c]	1.83	81	2.18	96
AGLA[b]	1.46	64	2.14	94
AGLB[c]	1.46	64	2.14	94
U-10	1.77	78	2.18	96
M1-2	1.59	70	1.99	88
U-4	1.90	84	2.16	95
AG plus 2 w/o tantalum	--	--	2.18	--
AG plus 5 w/o tantalum	--	--	2.24	--
AG plus 10 w/o tantalum	--	--	2.33	--

Table 2. (Continued)

Specimen[a]	Density After Cold Hydrostatic Pressing		Density After Hot Isostatic Compaction	
	G per Cm^3	Per Cent of Theoretical	G per Cm^3	Per Cent of Theoretical
Isostatically Hot Pressed at 2700 C and 1600 Atm for 1 Hr				
A-6	1.46	64	2.24	99
M3-2	1.71	76	2.12	93
C-5	1.97	87	2.03	90
A-1	1.34	59	2.15	95
U-6	2.03	90	2.18	96
U-5	2.09	92	2.22	98

(a) Numbers correspond to those in Table 1.
(b) Specimens cut longitudinally (cylindrical axes parallel).
(c) Specimens cut transversely (cylindrical axes perpendicular).

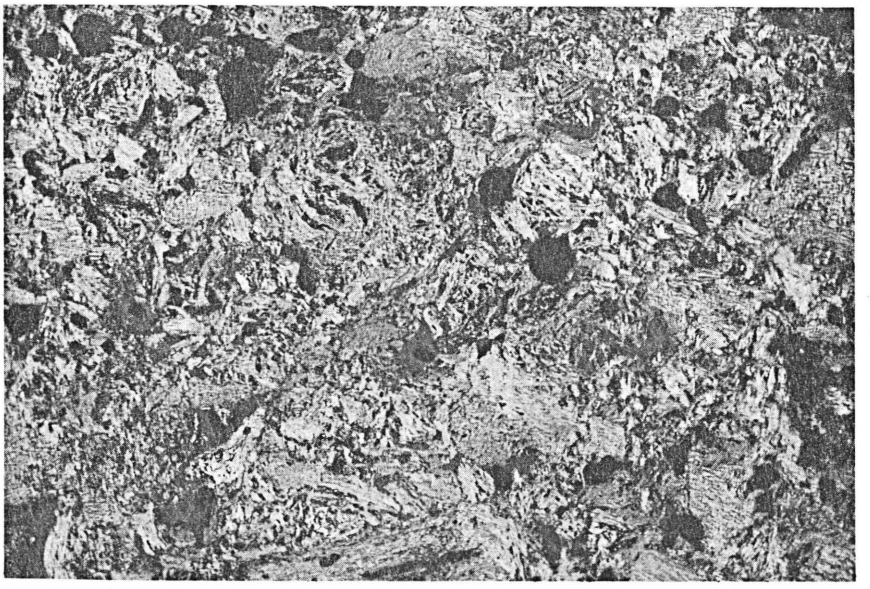

100X RM18397

FIGURE 6. REPRESENTATIVE MICROSTRUCTURE OF CONVENTIONALLY FABRICATED REACTOR-GRADE GRAPHITE

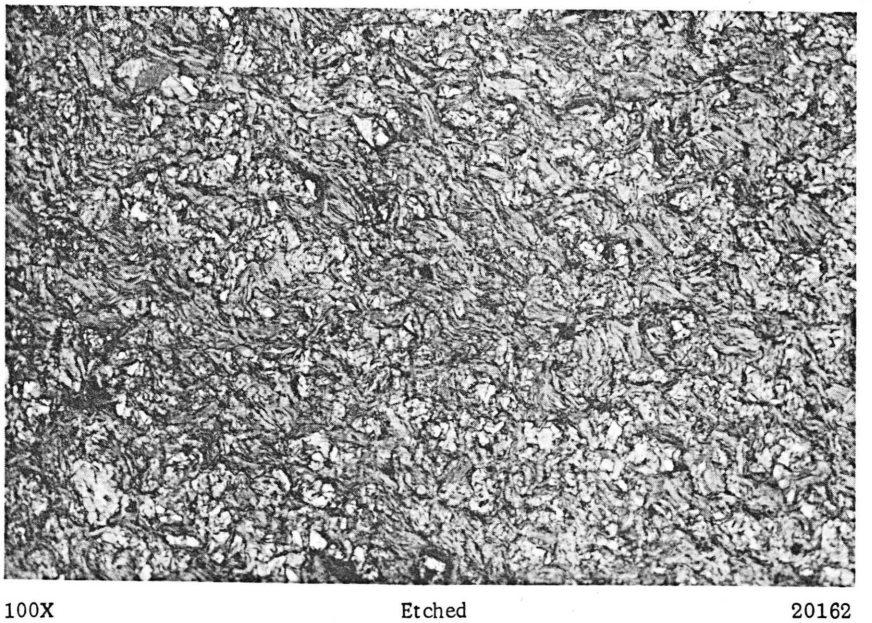

100X Etched 20162

FIGURE 7. NORWEGIAN NATURAL-GRAPHITE POWDER HOT ISOSTATICALLY COMPACTED AT 1750 C AND 1090 ATM TO A DENSITY OF 2.18 G PER CM^3

Specimen N-2 is shown here.

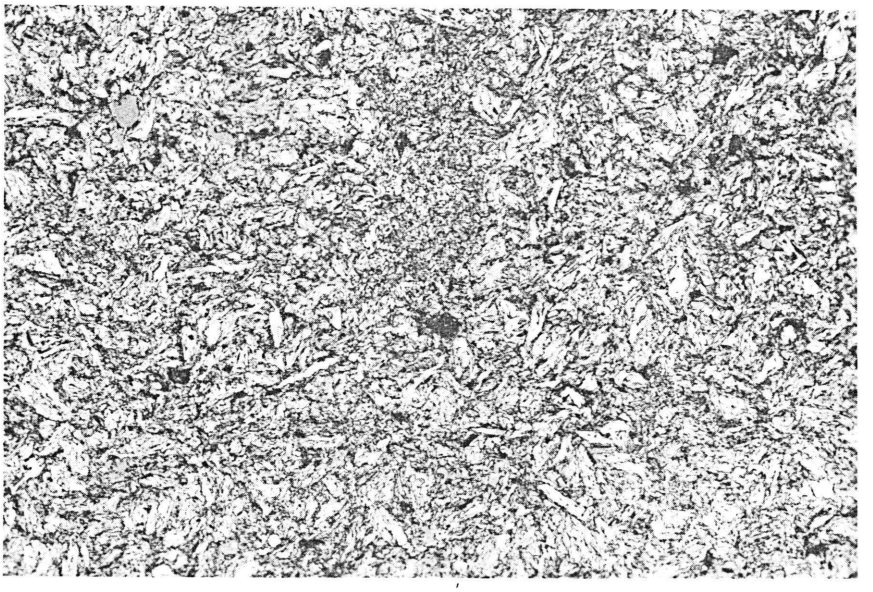

100X Etched 21301

FIGURE 8. CEYLONESE NATURAL-GRAPHITE POWDER HOT ISOSTATICALLY COMPACTED AT 2700 C AND 820 ATM TO A DENSITY OF 2.09 G PER CM^3

Specimen C-5 is shown here.

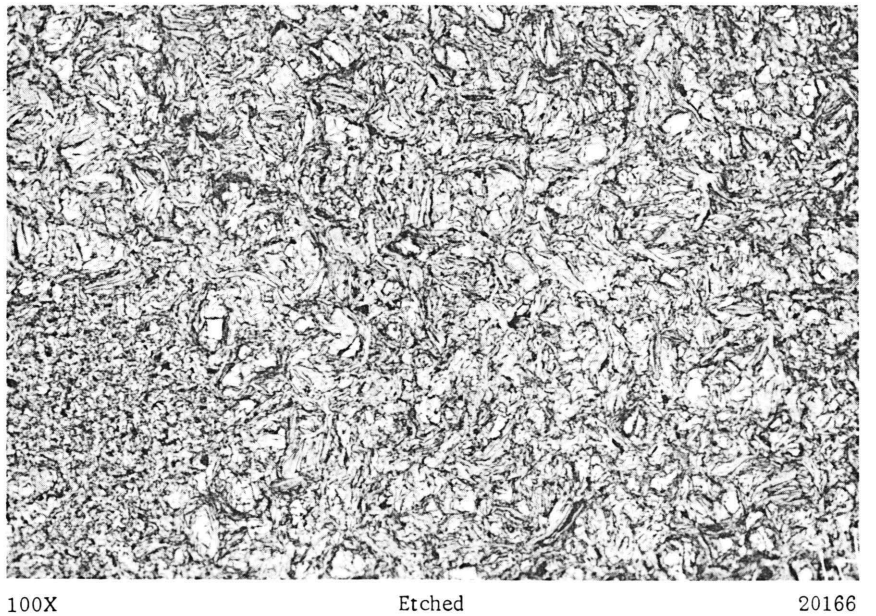

100X Etched 20166

FIGURE 9. MADAGASCAN NATURAL-GRAPHITE POWDER HOT ISOSTATICALLY COMPACTED AT 1750 C AND 1090 ATM TO A DENSITY OF 2.14 G PER CM^3

Specimen Ma-4 is shown here.

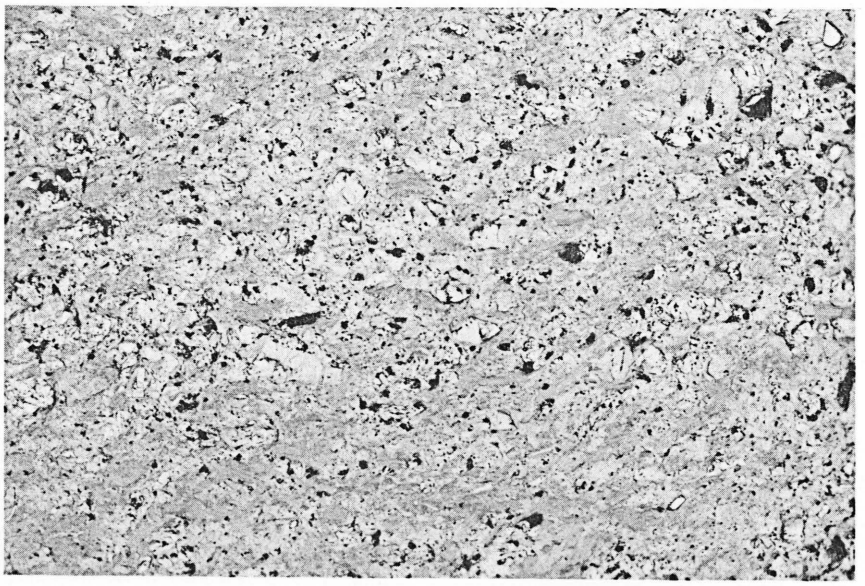

100X 17397

FIGURE 10. SPECTROGRAPHIC-GRADE GRAPHITE POWDER HOT ISOSTATICALLY COMPACTED AT 1650 C AND 680 ATM TO A DENSITY OF 2.08 G PER CM^3

Specimen U-3 is shown here.

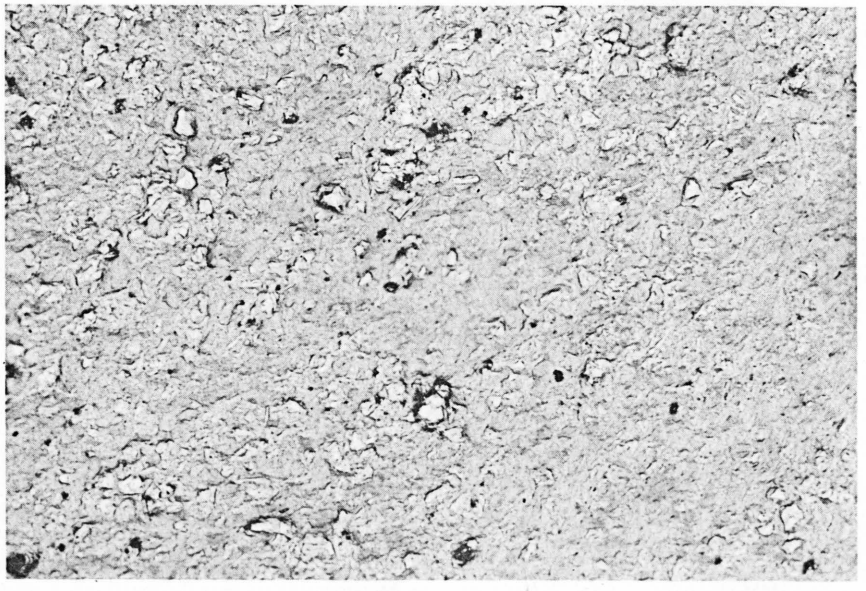

100X 17395

FIGURE 11. SPECTROGRAPHIC-GRADE GRAPHITE POWDER HOT ISOSTATICALLY COMPACTED AT 1950 C AND 2040 ATM TO A DENSITY OF 2.18 G PER CM^3

Specimen U-2 is shown here.

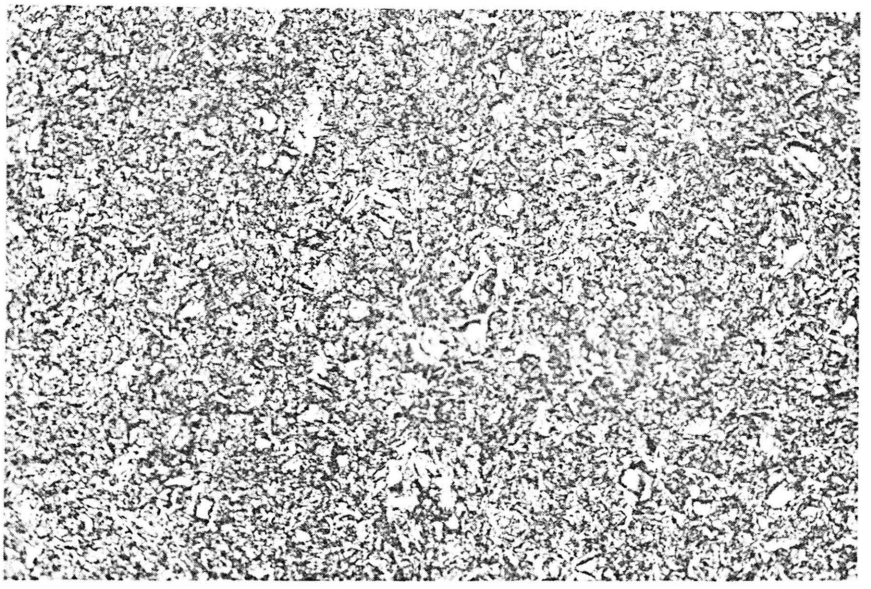

100X Etched 21328

FIGURE 12. SPECTROGRAPHIC-GRADE GRAPHITE POWDER HOT ISOSTATICALLY COMPACTED AT 2700 C AND 820 ATM TO A DENSITY OF 2.18 G PER CM^3

Specimen U-10 is shown here.

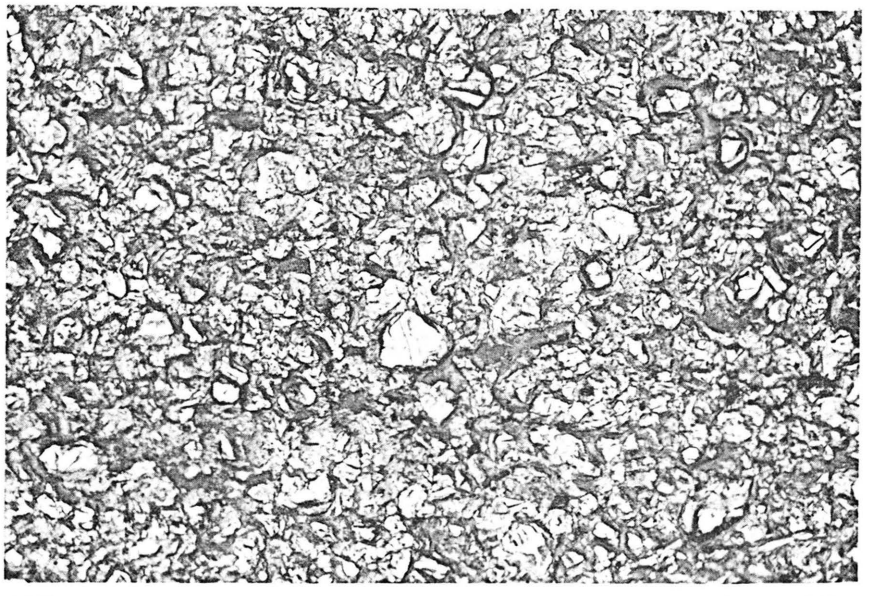

100X 18703

FIGURE 13. SPECTROGRAPHIC-GRADE GRAPHITE POWDER HOT ISOSTATICALLY COMPACTED AT 2700 C AND 1600 ATM TO A DENSITY OF 2.22 G PER CM^3

Specimen U-5 is shown here.

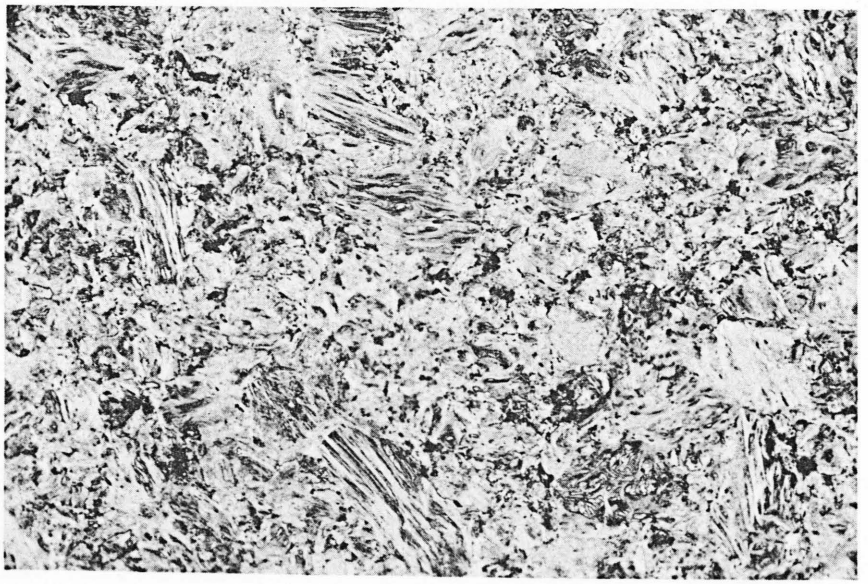

100X Etched 21309

FIGURE 14. PURE ARTIFICIAL-GRADE GRAPHITE POWDER HOT ISOSTATICALLY COMPACTED AT 2700 C AND 820 ATM TO A DENSITY OF 2.10 G PER CM^3

Specimen A-6 is shown here.

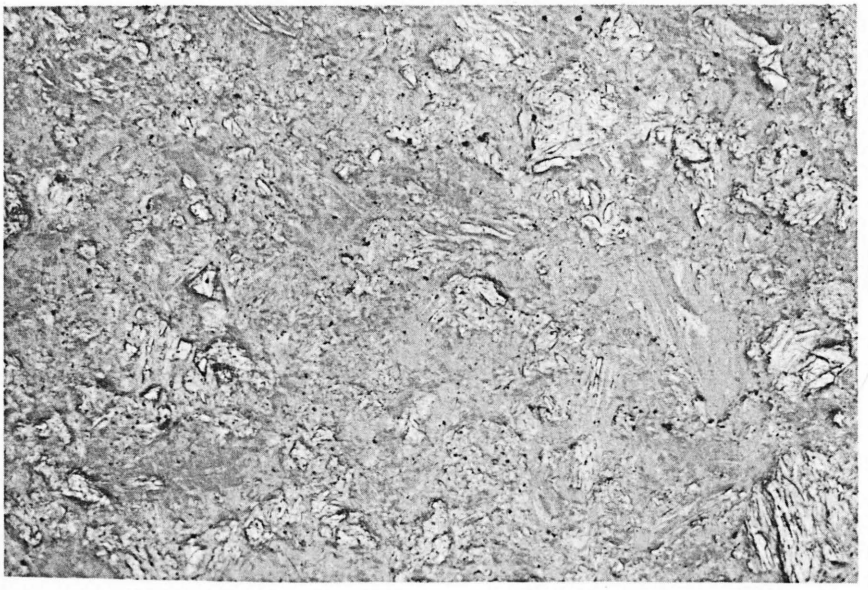

100X 18702

FIGURE 15. PURE ARTIFICIAL-GRADE GRAPHITE POWDER HOT ISOSTATICALLY COMPACTED AT 2700 C AND ~~1600~~ ATM TO A DENSITY OF 2.24 G PER CM^3

Specimen A-6 is shown here.

Isotropy Analysis by Neutron Diffraction

Neutron diffraction provided a useful tool for measuring the orientation of the graphite specimens. Neutrons are not scattered by electrons as are X-rays, but by the atomic nuclei. The scattering of neutrons by an element is not simply dependent upon its atomic number (the number of electrons), or its position in the periodic table, or its chemical properties, but is a more complex function which must be measured empirically for each element. The scattering cross section for graphite is reasonably large even though it has a low atomic number. The linear absorption coefficient (μ) of graphite is a great deal less for neutrons than for electrons; i. e., for neutrons of λ = 1.08 A, μ = 0.005 cm^{-1}, whereas for X-rays of λ = 1.54 A, μ = 19.2 cm^{-1}.[11] $I_x = I_o\, e^{-\mu x}$, where I_o = intensity of incident beam and I_x = intensity of transmitted beam passing through a thickness, x. The transmission (which is a function of both true absorption and scattering) for a 1/4-in. -thick graphite specimen is 80 per cent for neutrons of 1.08 A and 0.25 per cent for X-rays of 1.54 A.[10] Therefore, neutrons penetrate much deeper into the bulk material than X-rays and are able to give more information than that just concerning structure on the surface. Because of the extreme anisotropy of graphite crystallites, almost any shaping operation (i. e., machining) tends to orient the surface differently from that of the bulk; therefore, a bulk orientation measurement is desirable.

Intensities of the (002) and (100)(101) reflections were measured at the Battelle Research Reactor using 1.05-A neutrons. Figure 16 shows a schematic diagram of the neutron-diffraction apparatus, which, in principle, is directly analogous to an X-ray diffraction apparatus. A photograph of the equipment at the Battelle Research Reactor is given in Figure 17. The integrated intensities of the diffraction peaks from these planes, which were measured both with the specimen cylinder axis perpendicular to (i. e., vertical, and designated as V) and parallel with (i. e., horizontal, and designated as H) the plane of reflection, give an indication of the degree of isotropy. In the latter case, the cylinder axis bisected the angle between the neutron source and the detector.

For neutron diffraction of powders, the intensity of the reflected beam, p, is given by

$$p = K\alpha \frac{jF^2}{\sin\theta \sin 2\theta} e^{-2w} A_{hk\ell}\, \rho(\beta)$$

for a cylindrical sample, where

K = a geometrical factor

α = a density factor which is a constant for a given specimen

j = multiplicity

θ = Bragg angle

F = structure amplitude factor

e^{-w} = Debye-Waller temperature factor

$A_{hk\ell}$ = absorption factor

$\rho(\beta)$ = the probability of finding a particular $hk\ell$ in a direction, β, measured from some reference position in the sample.

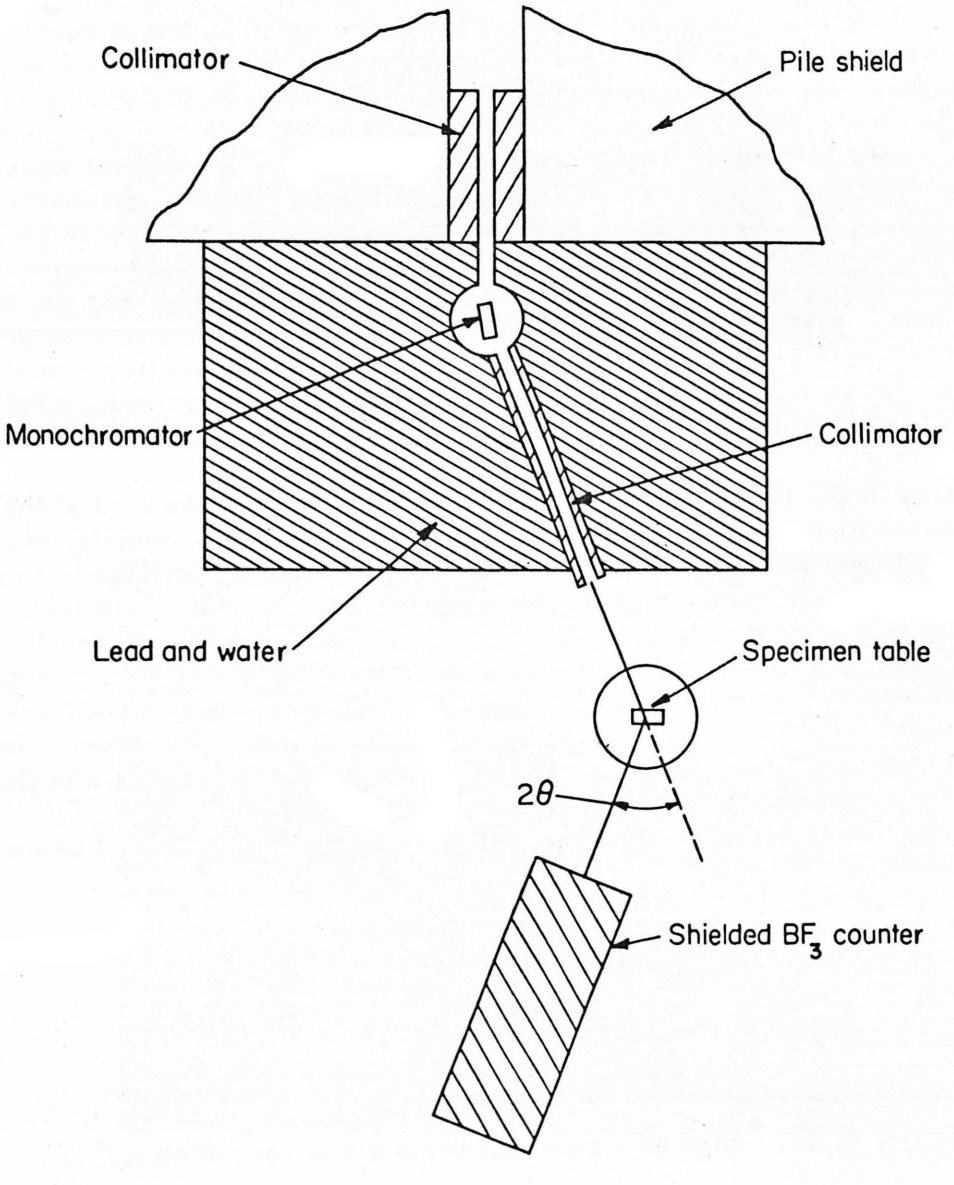

FIGURE 16. SCHEMATIC DIAGRAM OF NEUTRON DIFFRACTION APPARATUS

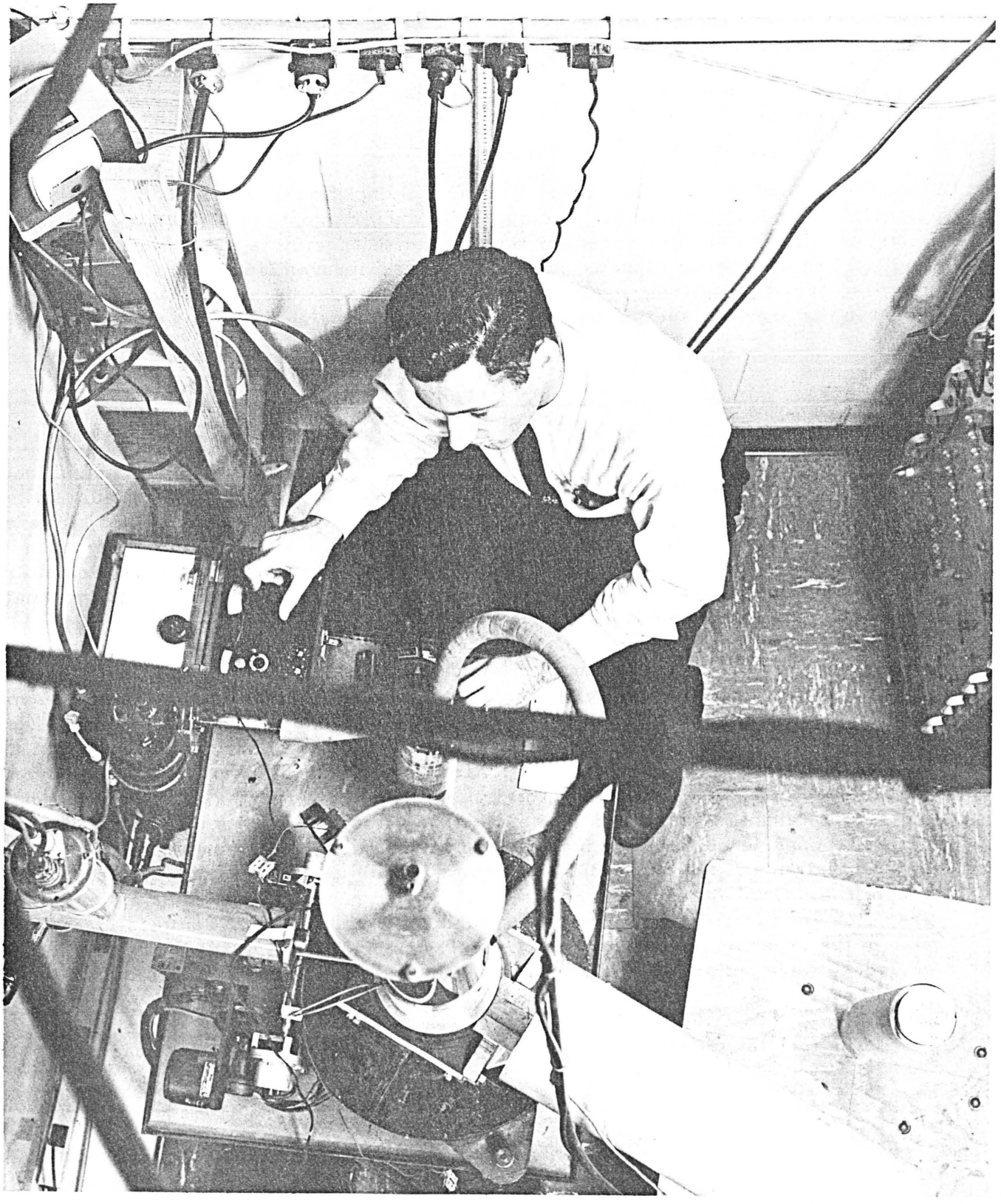

86043

FIGURE 17. PHOTOGRAPH OF THE NEUTRON DIFFRACTION EQUIPMENT AT THE BATTELLE RESEARCH REACTOR

For these experiments, β is either 0 deg or 90 deg (H or V) if the cylinder axis is used as a reference pole. The ratio of the $K\alpha jF^2_{(002)}$ values in the two directions (V and H) is therefore the ratio of the probabilities, $\rho(90)/\rho(0)$, of finding (002) poles in the two directions and would be equal to unity for ideal isotropy. It was necessary to use the sum of the intensities for the (100) and (101) planes in the ratios since resolution of these reflections was not possible. This ratio, $\frac{jF^2(002)}{jF^2(100)(101)}$, would have a value of 0.760 in the ideally random, isotropic case. But by dividing the experimental ratio by the value calculated for isotropy (0.760), a comparable factor is obtained which is unity for ideal isotropy. The values measured for the compacted specimens are presented in Tables 3 and 4. The specimens reported in Table 4 show improved isotropy as a result of the omitting of tamping during the original loading of the powders into the rubber bags, as noted in the previous section on cold-hydrostatic-pressing procedures.

Tensile-Strength Measurements

An indirect method for determining tensile strength, called the diametral loading technique, was used. It consists of compression loading short, right circular cylinders across a diameter. The specimens break perpendicular to the applied load, in tension along the loaded diameter. Although the practical test deviates somewhat from the ideal used to develop the theory, its use for testing the tensile strength of ceramic materials has been justified by its reasonable accuracy, simplicity, and convenience for small specimens and has been adequately treated in the literature.[11, 12] Two aspects of brittle-fracture theory might appropriately be considered when interpreting the results of these tests. First, the strength of brittle materials should be described statistically to be most meaningful. In general, this was not possible here due to the small number of specimens available for each set of conditions. Second, all experimental methods of measuring fracture strength involve experimental difficulties and peculiarities (i.e., variations in stress distributions and errors introduced by gripping, holding, or crushing the specimen, specimen size, etc.); therefore, the strengths determined by different techniques cannot be compared with each other without reservation. In addition, graphite cannot be considered to be the ideal brittle material. Notwithstanding the reservations in interpretation of the data, this technique is useful as a simple tensile test for small specimens. Good agreement was obtained between published strengths of commercial graphites and those determined by this technique on commercial samples identical in size to the experimental samples. The test variables, i.e., loading rate and loading surfaces, were optimized on the equipment by the use of the commercial graphite cylinders.

The tensile strength is calculated from the applied compressive load by

$$\sigma = \frac{2P}{\pi d \ell}$$

where

P = the applied load

d = specimen diameter

ℓ = specimen length.

TABLE 3. ORIENTATION OF COMPACTED GRAPHITE SPECIMENS BY NEUTRON DIFFRACTION PRIOR TO INCORPORATION OF PROCEDURES TO IMPROVE ISOTROPY OF COLD-PACKED POWDERS

Sample	Type of Cut[a]	Cylinder Axis[b]	Plane	Intensity, ($\alpha K j F^2$)	Relative Intensity, $\left[\frac{F^2(002)_V}{F^2(002)_H}\right]$[c]	Orientation Factor $\left[\frac{jF^2(002)}{jF^2(100)(101)}\right]$[d]	
						Experimental Value	Ratio of Experimental to Calculated Values[e]
Graph-i-tite A	Longitudinal	Vertical	(002)	0.647	1.658	0.954	1.2555
		Vertical	(100)(101)	0.678	--	--	--
		Horizontal	(002)	0.390	--	0.454	0.596
		Horizontal	(100)(101)	0.859	--	--	--
AGOT	Longitudinal	Vertical	(002)	0.569	1.977	1.130	1.487
		Vertical	(100)(101)	0.503	--	--	--
		Horizontal	(002)	0.288	--	0.332	0.437
		Horizontal	(100)(101)	0.867	--	--	--
AGR	Longitudinal	Vertical	(002)	0.693	4.801	1.621	2.133
		Vertical	(100)(101)	0.425	--	--	--
		Horizontal	(002)	0.144	--	0.191	0.252
		Horizontal	(100)(101)	0.755	--	--	--
U-2	Longitudinal	Vertical	(002)	0.332	0.205	0.197	0.259
		Vertical	(100)(101)	1.686	--	--	--
		Horizontal	(002)	1.618	--	2.512	3.305
		Horizontal	(100)(101)	0.644	--	--	--
U-5	Longitudinal	Vertical	(002)	0.218	0.0353	0.112	0.147
		Vertical	(100)(101)	1.952	--	--	--
		Horizontal	(002)	1.176	--	14.04	18.47
		Horizontal	(100)(101)	0.440	--	--	--
A-6	Longitudinal	Vertical	(002)	0.488	1.291	0.836	1.100
		Vertical	(100)(101)	0.584	--	--	--
		Horizontal	(002)	0.378	--	0.604	7.95
		Horizontal	(100)(101)	0.626	--	--	--
M-1	Longitudinal	Vertical	(002)	0.544	0.829	0.695	0.920
		Vertical	(100)(101)	0.779	--	--	--
		Horizontal	(002)	0.656	--	1.219	1.604
		Horizontal	(100)(101)		--	--	--

(a) Longitudinal denotes that diffraction sample was cut so that its cylinder axis was parallel with the original cylinder axis of the specimen.

(b) Position of the sample in the neutron beam.

(c) This value could vary from zero to infinity and would be unity in the ideally random, isotropic case.

(d) This value would be 0.760 in the ideally random, isotropic case.

(e) Same orientation factor as in previous column. Values of ratio could vary from zero to infinity and would be unity in the ideally random, isotropic case.

TABLE 4. ORIENTATION OF COMPACTED GRAPHITE CYLINDERS BY NEUTRON DIFFRACTION AFTER CHANGING POWDER LOADING TECHNIQUE TO INCREASE ISOTROPY

Sample	Type of Cut[a]	Cylinder Axis[b]	Plane	Intensity, ($\alpha K j F^2$)	Relative Intensity in Direction Shown: $\left[\frac{F^2(002)_V}{F^2(002)_H}\right]$[c]	Relative Intensity in Direction Shown: $\left[\frac{F^2(002)\text{long., H}}{F^2(002)\text{trans., H}}\right]$[c]	Relative Intensity in Direction Shown: $\left[\frac{F^2(002)\text{long., V}}{F^2(002)\text{trans., V}}\right]$[c]	Orientation Factor $\left[\frac{jF^2(002)}{jF^2(100)(101)}\right]$[d]: Experimental Value	Orientation Factor $\left[\frac{jF^2(002)}{jF^2(100)(101)}\right]$[d]: Ratio of Experimental to Calculated Values[e]
AGL	Longitudinal	Vertical	(002)	0.540	0.584	--	0.695	0.578	0.761
		Vertical	(100)(101)	0.935	--	--	--	--	--
		Horizontal	(002)	0.924	--	1.249	--	1.173	1.543
		Horizontal	(100)(101)	0.788	--	--	--	--	--
	Transverse	Vertical	(002)	0.778	1.052	--	--	1.047	1.378
		Vertical	(100)(101)	0.744	--	--	--	--	--
		Horizontal	(002)	0.740	--	--	--	0.747	0.923
		Horizontal	(100)(101)	0.991	--	--	--	--	--
U-13L	Longitudinal	Vertical	(002)	0.656	0.596	--	1.055	0.688	0.905
		Vertical	(100)(101)	0.952	--	--	--	--	--
		Horizontal	(002)	1.100	--	0.408	--	1.287	1.693
		Horizontal	(100)(101)	0.855	--	--	--	--	--
	Transverse	Vertical	(002)	0.692	1.540	--	--	0.642	0.845
		Vertical	(100)(101)	1.077	--	--	--	--	--
		Horizontal	(002)	0.449	--	--	--	0.366	0.482
		Horizontal	(100)(101)	1.227	--	--	--	--	--
MC-2	Longitudinal	Vertical	(002)	0.654	0.880	--	--	0.651	0.857
		Vertical	(100)(101)	1.050	--	--	--	--	--
		Horizontal	(002)	0.743	--	--	--	0.828	1.089
		Horizontal	(100)(101)	0.897	--	--	--	--	--
MG-2	Longitudinal	Vertical	(002)	0.648	0.724	--	--	0.633	0.833
		Vertical	(100)(101)	1.023	--	--	--	--	--
		Horizontal	(002)	0.894	--	--	--	1.085	1.428
		Horizontal	(100)(101)	0.825	--	--	--	--	--

(a) Longitudinal denotes that diffraction sample was cut so that its cylinder axis was parallel with the original cylinder axis of the specimen; transverse denotes that diffraction sample was cut so that its cylinder axis was perpendicular to the original cylinder axis of the specimen.

(b) Position of the sample in the neutron beam.

(c) This value could vary from zero to infinity and would be unity in the ideally random, isotropic case.

(d) This value would be 0.760 in the ideally random, isotropic case.

(e) Same orientation factor as in previous column. Values of ratio could vary from zero to infinity and would be unity in the ideally random, isotropic case.

The tensile strengths measured by the diametral compression tests in this study are detailed in Table 5, in which the pronounced effects of both the base powder materials and the compaction parameters are apparent. For comparison, values obtained for several commercial graphite materials are included at the top of the table. Since neutron-diffraction analysis was performed on the specimens in this program prior to the strength tests, the lack of effect of this procedure was confirmed on the commercial materials, as can be noted in the table.

DISCUSSION OF RESULTS

The results of the experiments indicated the hot-isostatic-compaction conditions of temperature, pressure, and time which are necessary for achieving high-density graphite structures from a variety of starting graphite powder materials without impregnation. A summary of the effect of compaction conditions on the densities of the various graphites is given in Table 6. The differences in results obtained with the different materials are readily apparent. In general, lower densities were obtained with the less pure graphite powders, such as the Mexican natural graphite (85 w/o carbon). Densities in the range of 95 per cent of theoretical (2.15 g per cm^3) were achieved from most of the higher purity materials at conditions of 1950 C and 2040 atm to 2700 C and 1600 atm for 1 to 2 hr. High-purity artificial and ultrahigh-purity spectrographic-grade graphites were densified to 98 to 99 per cent of theoretical (>2.20 g per cm^3) at 2700 C and 1600 atm.

The temperature-limiting factor of the hot-isostatic-compaction process using tantalum containers to transmit the pressure to the graphite powder is the tantalum-carbon eutectic temperature of ~2800 C. At 2700 C the maximum pressure presently obtainable for practical operation of the equipment is 1600 atm.

The microstructure of densified graphites from various powder sources varied widely, as shown in Figures 7 through 15. The measured high densities of the hot-isostatically-compacted specimens were confirmed by reflected-light microscopy techniques. The commercial graphite structure presented in Figure 6 should be compared with the higher density structures of the isostatically compacted materials shown in Figures 7 through 15. The effects of increasing pressure and temperature on the density of spectrographic-grade graphite compacts is illustrated by Figures 10 through 13.

Because of their platelike particle shape, some of the powders assumed a rather high degree of orientation during the loading prior to compaction. The pyrolytic-graphite specimens were extreme examples of this type of orientation. In this case, the orientation was so severe that delaminations caused sample crumbling before any density, strength, or neutron-diffraction measurements could be made on this type of specimen. Another example of orientation occurred in the spectrographic specimens, i.e., U-2 and U-5. Although this anisotropy is not so apparent in the photomicrographs (Figures 10 through 13) these platelike particles lined up with their (002) planes perpendicular to the specimen cylinder axis. This is illustrated for Specimens U-2 and U-5 by the neutron-diffraction data in Table 3. As shown in Table 4, this type of orientation was reduced by changing the cold-loading procedures for the powders.

The artificial graphite specimens were very nearly isotropic and are of particular interest in this regard. Specimen A-6 (Table 3) is an example of such an isotropic

TABLE 5. TENSILE STRENGTH OF GRAPHITE CYLINDERS DETERMINED BY THE DIAMETRAL COMPRESSION TEST

Specimen[a]	Density, g per cm^3	Density, per cent of theoretical	Mean Calculated Tensile Strength, psi	Number of Specimens Tested
Commercial Extruded Graphites				
Graph-i-tite A	1.90	84	2150	10
AGOT	1.65	73	1534	10
AGOT[b] after neutron diffraction testing	1.65	73	1494	4
AGR	1.65	73	1000	10
AGR[b] after neutron diffraction testing	1.65	73	1110	6
AGR after heat treatment at >2500 C	1.54	64	906	10
Isostatically Hot Pressed at 1650 C and 680 Atm for 2 Hr				
M-4	1.84	81	1160	2
M-6	1.91	84	2250	1
C-6[c]	2.08	92	201	1
Isostatically Hot Pressed at 1750 C and 1090 Atm for 2 Hr				
N-1[c]	2.13	94	606	2
M-3	1.95	86	1993	2
N-2	2.18	96	881	1
Ma-4	2.14	94	885	2
Isostatically Hot Pressed at 1950 C and 2040 Atm for 2 Hr				
U-2[b]	2.18	96	234	2
M-1[b]	2.03	90	2048	2
M-2	2.12	93	3530	1
N-7	2.24	99	447	1
C-7	2.15	95	954	1
Isostatically Hot Pressed at 2500 C and 440 Atm for 2 Hr				
U-7	2.19	97	469	1
MC-2[b]	1.82	80	1819	1
MG-2[b]	1.87	82	995	1
A-3	1.95	86	484	1
M-7	1.67	74	1140	1
Ma-6	2.19	97	590	3
Isostatically Hot Pressed at 2700 C and 820 Atm for 1 Hr				
C-5	2.09	92	1013	1
N-6[c]	2.02	89	387	1
U-6	2.15	95	615	1
A-6	2.10	93	638	2
Ma-7[c]	1.83	81	878	1
MG-2	1.91	84	1037	1
U-13LA[b, d]	2.15	95	378	2
U-13LB[b, e]	2.18	96	360	2
AGLA[b, d]	2.14	94	907	3
AGLB[b, e]	2.14	94	885	3
U-10	2.18	96	769	1
Ma-a[c]	2.20	97	941	1
MI-2	1.99	88	1750	1
U-4	2.16	95	1127	2
AG plus 2 w/o tantalum	2.18	96	720	1

TABLE 5. (Continued)

Specimen[a]	Density, g per cm^3	Density, per cent of theoretical	Mean Calculated Tensile Strength, psi	Number of Specimens Tested
AG plus 5 w/o tantalum	2.24	99	814	1
AG plus 10 w/o tantalum	2.33	103	965	1
Isostatically Hot Pressed at 2700 C and 1600 Atm for 1 Hr				
A-6[b]	2.24	99	887	1
C-2	1.92	85	214	1
N-6	2.13	94	696	2
M3-2	2.12	93	2787	3
C-5	2.03	90	527	2
A-1	2.15	95	750	1
Ma-7	2.03	90	1008	1
U-6	2.18	96	520	1

(a) Numbers correspond to those in Table 1.
(b) Specimens which were used for neutron-diffraction orientation determination.
(c) Container leak during hot compaction caused density decrease.
(d) Specimens cut longitudinally (cylindrical axes parallel).
(e) Specimens cut transversely (cylindrical axes perpendicular).

TABLE 6. DENSITY OF HOT-ISOSTATICALLY-COMPACTED GRAPHITES DENSIFIED AT VARIOUS CONDITIONS

	Density Obtained at Hot-Isostatic-Compaction Conditions Shown, per cent of theoretical						
	2 Hr at 1650 C and 680 Atm	2 Hr at 1750 C and 1090 Atm	2 Hr at 1950 C and 2040 Atm	2 Hr at 2500 C and 440 Atm	1 Hr at 2700 C and 820 Atm	1 Hr at 2700 C and 1600 Atm	Commercial Material[a]
Artificial grade	--	--	--	86	94	99	--
Spectrographic grade	92	--	96	97	96	98	--
Natural grades							
Mexican	84	86	91	--	--	93	--
Ceylonese	--	--	95	--	92	--	--
Norwegian	--	96	99	--	--	--	--
Madagascan	--	94	--	97	--	--	--
Carbon mixture	--	--	--	80	--	--	--
Graphite mixture	--	--	--	82	84	--	--
Commercial grades							
AGR	--	--	--	--	--	--	73
AGOT	--	--	--	--	--	--	73
Graph-i-tite A	--	--	--	--	--	--	84

(a) Typical commercial graphites.

specimen produced by this technique. A photomicrograph of this specimen is shown in Figure 15.

A summary of the tensile strengths determined by the diametral loading test of specimens produced at different compaction conditions using various materials is presented in Table 7. The constraints on strength-data interpretation were discussed earlier. In general, it can be noted in Table 7 that the strength of the hot-isostatically-compacted graphites is moderate and comparable to that of ordinary commercial graphites. It can also be observed that the specimens compacted from the lower purity natural-graphite powders have generally higher strengths. With regard to the results, it should be considered that the strength of these hot-isostatically-compacted materials must be dependent upon their isotropy, and it is significant that limited tests of the relatively isotropic materials showed equal strengths in both principal directions.

The unique, very dense, and relatively isotropic graphite materials prepared in this investigation are to be characterized more completely in continuing studies, and specimens will be prepared for irradiation testing. A pure artificial-grade powder and a pure natural-grade powder will be evaluated as representative starting materials of interest. Only limited additional studies will be conducted of material variables. Evaluations of the isostatically compacted products will include multiple specimens and tests to characterize the isotropy, tensile strength, density, type of porosity, microstructure, thermal expansion, permeability, and thermal-cycling behavior. Specimens of the characterized graphites will then be prepared for irradiation testing at Battelle-Northwest to obtain information on the behavior of this unique type of material and to provide further insight into the behavior mechanisms of graphite under irradiation.

CONCLUSIONS

From the results of this study it can be concluded that:

(1) Very high densities (up to 2.24 g per cm^3 or 99 per cent of theoretical) can be obtained by hot isostatically compacting powders of high-purity artificial graphite and ultrahigh-purity spectrographic graphite at 2700 C and 1600 atm.

(2) Essentially isotropic graphite can be obtained by hot isostatically compacting artificial graphite powder. Both starting materials and process parameters significantly influence the degree of isotropy obtainable.

(3) The strength of hot isostatically compacted graphite does not differ significantly from that of commercial materials, but the relatively isotropic materials showed equal strengths in both directions.

(4) Owing to its very high density and relatively high isotropy, the hot isostatically compacted material appears worthy of continued characterization studies and irradiation evaluation.

TABLE 7. TENSILE STRENGTH OF GRAPHITE CYLINDERS COMPACTED AT DIFFERENT CONDITIONS[a]

	Tensile Strength of Specimens Hot Isostatically Compacted at Conditions Shown, psi						
	2 Hr at 1650 C and 680 Atm	2 Hr at 1750 C and 1090 Atm	2 Hr at 1950 C and 2040 Atm	2 Hr at 2500 C and 440 Atm	1 Hr at 2700 C and 820 Atm	1 Hr at 2700 C and 1600 Atm	Commercial Material[b]
Artificial grade	--	--	--	500	900	900	--
Spectrographic grade	--	--	200	500	1000	--	--
Natural grades							
Mexican	1700	2000	3500	1100	1800	3000	--
Ceylonese	--	--	1000	--	1000	--	--
Norwegian	--	700	500	--	--	700	--
Madagascan	--	900	--	600	--	1000	--
German	--	--	1400	--	--	--	--
Carbon mixture	--	--	--	1800	--	--	--
Graphite mixture	--	--	--	1000	--	--	--
Commercial grades							
AGR	--	--	--	--	--	--	1100
AGOT	--	--	--	--	--	--	1500
Graph-i-tite A	--	--	--	--	--	--	2200

(a) Tensile strengths were measured by the diametral loading technique.

(b) Typical tensile strengths of commercial graphites.

ACKNOWLEDGMENTS

This investigation was conducted under the sponsorship of the Fuels and Materials Development Branch, Division of Reactor Development and Technology of the Atomic Energy Commission. The helpful guidance of Mr. Jack G. Conner of the AEC in the conduct of this study is acknowledged. The authors also wish to thank Mr. C. B. Boyer, Mr. E. Adelson, and Mr. M. C. Brockway of Battelle for their assistance in this work.

REFERENCES

(1) De Halas, D. R., Nuclear Graphite, Chapter 7, Academic Press, New York (1962).

(2) Anderson, A. I., et al., "Advanced Course on In-Core Instrumentation for Water-Cooled Reactors", lecture notes from the Netherlands-Norwegian Reactor School (August 21 to September 1, 1961).

(3) Gray, B. S., et al., "Mechanism of Radiation Induced Contraction in Polycrystalline Graphite"; Helm, J. W., "Radiation Effects in Graphite at High Temperatures". Presented at Seventh Biennial Conference on Carbon, Cleveland, June 21 to 25, 1965.

(4) Paprocki, S. J., et al., "Progress on the Use of Gas-Pressure Bonding for Fabricating Low-Cost Ceramic, Cermet, and Dispersion Fuels", BMI-1475 (November, 1960).

(5) Porembka, S. W., "Gas Pressure Bonding", Ceram. Age (November, 1963).

(6) Boyer, C. B., and Conaway, M. R., "High Temperature, High Pressure Hot-Isostatic Compaction Equipment", to be published.

(7) McGeary, R. K., J. Am. Ceram. Soc., 44 (10), 513-522 (1961).

(8) Tarpinian, Aram, and Gozza, G. E., "A Technique for Microstructural Examination of Polycrystalline Graphites", WAL-TR-132.5/1 (February, 1959).

(9) Tarpinian, Aram, "Electrochemical and Ion Bombardment Etching of Pyrolytic Graphite", J. Am. Ceram. Soc., 47 (10), 532 (1964).

(10) Bacon, G. E., Neutron Diffraction, Oxford University Press (1955).

(11) Ownby, P. D., "A Preliminary Study of the Effect of Heat Treatment on the Strength and Microstructure of a Glass-Ceramic Material", M.S. thesis, Missouri School of Mines and Metallurgy (Rolla) (October, 1962).

(12) Rudnick, A., Hunter, A. R., and Holden, F. C., "An Analysis of the Diametral-Compression Test", Mater. Res. Std., 3 (4), 283-289 (April, 1963).

DCC:DPO:ESH/eh